Design, Fabrication and Characterization of an 8-inch X-HPD

André Braem [a], Christian Joram [a 1], Jacques Séguinot [a], Paola Solevi [b] and Anne-Gaelle Dehaine [c]

[a] *CERN, PH Department, Geneva, Switzerland*

[b] *ETH Zürich, Switzerland*

[c] *Photonis SAS, Brive-La-Gaillarde, France*

Abstract

The X-HPD is a modern implementation of the hybrid concept first employed by the Philips SMART and the QUSAR tubes of the Lake Baikal experiment, aiming at improved performance and maximum simplicity. The glass envelope is essentially spherical and a spatial scintillator crystal is mounted in its centre. Photoelectrons from the cathode are accelerated by a potential difference of 20-30 kV and deposit their kinetic energy in the scintillator (or Phosphor). The generated scintillation light is detected by a small and low cost photodetector, e.g. a conventional PMT. The spherical symmetry leads to a uniform collection efficiency and very small intrinsic time spread over the full viewing angle of 120° (3 π solid angle). We report about the design, fabrication and test results of a first X-HPD prototype of 208 mm diameter with a conical LYSO crystal anode. Monte-Carlo studies with Geant4 led to a qualitative understanding of the light transport in the anode assembly.

1. Introduction

In the framework of the C2GT design study [1] we developed the concept of a large (e.g. 15-inch diameter) almost spherical Hybrid Photodetector (HPD) with centrally placed anode. While the anode was originally foreseen to consist of Silicon sensors, mounted on a ceramic cube of 15 mm side length, we have now implemented a conceptually simpler alternative, namely a spatial scintillator crystal which is read out through a window by an external small PMT. This concept, which we gave the name *X-HPD*, is a modern implementation and extension of the *Dumand Smart PMT* [2] and *Lake Baikal Quasar* [3] approaches to large area photon detectors.

The readout of the scintillator can obviously be accomplished by other photodetectors, e.g. by Geiger mode APDs, as proposed in [4].

2. Concept and design of the X-HPD

An X-HPD consists of a glass sphere with a round opening which is sealed by a base plate. A scintillator crystal is mounted in the centre of the sphere, mechanically supported from the base plate, and serves as anode. A semi-transparent photocathode covers a large part ($\approx 3/4$) of the sphere. The electrical field between cathode and anode is radial ($E \sim 1/r^2$), apart from distortions in the vicinity of the anode support. A ring electrode, parallel to the edge of the photocathode area allows correcting for these distortions. The potential difference between cathode and anode is of the order 20-30 kV. Photoelectrons bombard the scintillator and create scintillation light, which is coupled to a small photodetector. For practical reasons, mainly for incompatibility with the vacuum bakeout process, the photodetector is mounted outside the vacuum sphere. The price to pay are light losses at the various interfaces crystal/window/light guide/photodetector. Particularly critical is the interface from crystal to window which involves a small vacuum gap. The scintillation photons have to pass an interface with high refractive index ratio ($\approx 1.8 : 1$) which unavoidably leads to substantial light losses. The scintillator is coated with a reflective, metallic coating, which has the function to define an equipotential surface and to avoid scintillation light leaking out of the crystal. The symmetry of the E-field allows in principle for imaging, i.e. it can be of interest for certain applications to segment the scintillator and also the photodetector. The scintillator crystal needs to have a minimum size to ensure a high hit probability for electrons from all regions of the photocathode. Its shape, e.g. cylindrical, hemi-spherical or conical has an impact on the optical characteristics of the anode (photon path lengths, number of reflections) and hence the final light yield.

The main advantages of the X-HPD concept are:

– Very large viewing angle. In practice the angle is limited by the geometry of the mechanical support of the crystal and the associated E-field distortions. Values of ±120°

are easily possible, corresponding to an active solid angle of 3π.
- Sensitivity increase due to a 'double cathode' effect. Light which traverses the semitransparent cathode unconverted has a second chance to be detected on the opposite side, then in reflective mode.
- Low transit time spread. The central position of the anode implies that the trajectories of all photoelectrons have in first approximation the same length. The flight time differences are in the sub-ns range.

In addition, there are a number of features, which the X-HPD shares with its predecessors, the Smart and Quasar tubes:
- The scintillation mechanism leads to a first stage gain of the order of 20-60, depending on the applied HV, choice of crystal and quality of light coupling. This results in a well defined signal, also for single photons, and a modest photon counting capability.
- The radial field geometry leads to immunity to the earth magnetic fielding and makes shielding obsolete.
- The tube is conceptionally simple and consists of very few components which should lead to competitive fabrication costs.

These features make the X-HPD concept a promising option for future large volume water based Cherenkov detectors, as underlined e.g. by studies in the framework of the KM3NeT project [5].

Our first fully operational X-HPD tube is based on a glass sphere of 208 mm external diameter (8 inches) and was fabricated in the CERN photocathode facility [6]. Earlier studies concerning the choice of the anode material and a first sealed tube with metal anode are described in [7,8]. The anode assembly (see Fig. 1) consists of a LYSO crystal of 12 mm diameter and 18 mm height and a glass cylinder with a thin flat window which is joint to the tubes base plate. The upper part of the LYSO crystal is tapered with an angle of 60° leaving a flat top of 3 mm diameter. The crystal is coated with a reflective Al film of 100 nm thickness. A light guide, made of an Al-coated truncated plexiglass cone ensures the optical contact between the window and the PMT tube of 25 mm diameter [2]. Fig. 2 shows a photo of the completed X-HPD.

3. Modelling of the light transport in the anode assembly

The choice of the scintillator crystal, its geometry and the way it is coupled to the photosensor have a crucial impact on the achievable light yield, i.e. the primary gain of the anode. At the time of the processing of the X-HPD described in this article, a series of systematic studies with Geant4[9] was launched to obtain first a qualitative and subsequently a quantitative understanding of the light yield for different anode geometries. Geant4 is a multi–purpose Monte Carlo tool for the simulation of passage of particles through matter in a wide energy range. The Geant4 electromagnetic physics package manages the electromagnetic interactions of leptons, photons, hadrons and ions, and provides specific code for optical photon transport. Optical photons can undergo in-flight absorption, elastic scattering (Rayleigh) and medium boundary interactions. The properties of media and surfaces relevant for the optical photon tracking can be assigned to a specific material, volume or interface between volumes, and modelled as a function of the wavelength. In this study, electrons of 20 keV energy interact in the crystal by depositing either their full or partial energy, according to the backscattering coefficient. Three geometries were studied: (1) a LYSO crystal of the above described shape and dimensions, (2) a hemispherical LYSO crystal of 12 mm diameter, and (3) an anode assembly based on a thin layer of Phosphor (e.g. P47) [3], deposited on a hemispherical glass window. The scintillation yields were assumed to be 30 photons/keV for LYSO and 10 photons/keV for P47 Phophor. Photons are considered as detectable when they pass the crystal/vacuum interface and hit a detection plane 1 mm below. Geometry (3) requires a hemispherical PMT for optimal geometrical matching [4]. The crystal and Phosphor surface are coated with a thin Al-layer and its specular and diffuse reflection properties are taken into account.

Fig. 3 summarizes the results of the Geant4 studies. The number of detectable photons is plotted versus the angle of incidence. While for the LYSO conical and hemispherical geometries the yield increases with the polar angle reaching a maximum of 200-250 photons for incidence from the top, the Phosphor geometry gives a constant yield of about 85 photons. The error bars correspond to the RMS fluctuations around the average value and are of the order 25% for the crystal geometries, i.e. significantly larger than what one would expect from Poisson statistics, while they are about 10% for the Phosphor geometry. The increased fluctuations for the crystals reflect the variety of different paths the photons can take before they escape from the crystal.

4. Fabrication and test of full X-HPD tubes

The X-HPD was processed in the CERN facility [6] with a standard bi-alkali photocathode. The anode assembly is prepared prior to the tube processing. The glass surfaces which are not covered by the photocathode were treated with a special UHV and high temperature compatible resistive coating [5] to avoid uncontrolled charging-up effects. After cathode deposition the tube was sealed in-situ with the base plate by means of a cold Indium press technique.

[2] Photonis XP3102, Gain $6 \cdot 10^6$ at 1000 V, P/V = 2.7

[3] Phosphor P47 is based on YSO scintillator grains embedded in a special lacquer.

[4] The 1-inch PMT XP31S2 from Photonis is well matched to the requirements.

[5] Details of the product and its processing fall under a non-disclosure agreement with the company Photonis SAS.

The PMT for the crystal readout was inserted into the glass cylinder only after the X-HPD is processed.

The tube can be powered either by applying negative HV to the photocathode and grounding the anode, or by applying positive HV to the anode and maintaining the cathode at ground. The latter configuration has the advantage that the field gradient between the corrector electrode ($U \approx -1$ kV) and the baseplate (ground) are very low.

The available time since the fabrication of the tube allowed to perform the following measurements:

- Relative sensitivity mapping as function of the polar angle. The tube was exposed to a blue LED (420 nm), operated in DC mode. The tube is polarized with positve HV (up to 5 kV) at the anode and the photocurrent extracted from the cathode is recorded with a picoamp meter.
- Pulse height and background measurements as a function of the applied HV (positive or negative). The tube was mounted in a test chamber and exposed to short light pulses from a self triggering H_2 flash lamp. Metal filters allowed to vary the light intensity from single to multiple photons. The signal from the PMT reading out the crystal was sampled by a charge sensitive ADC (gate length 100 or 125 ns) in a VME based readout system, triggered by a pick-up signal from the H_2 lamp.
- Polar angle scans with a pulsed blue LED. The measurement is performed in a large dark box. The readout is based on a fast digital oscilloscope.
- Timing measurements with a pulsed blue LED, also performed in the dark box. The LED has a time jitter of 1 ns.

4.1. *Results*

A first series of measurements performed with negative HV has been described in [10]. We report here about new measurements with positive HV and compare them to the earlier results. Fig. 4 shows the relative variation of the quantum efficiency of the photocathode for a polar angular scan from $-45°$ to $90°$ ($0°$ is the tube's equator). The *double cathode* effect is clearly visible, although the increase in QE is less expressed than previously observed for the metal-anode prototype [7], where an increase of a factor 2 was observed. We suspect that the earlier protoype tube had a particularly-thin photocathode which enhances the phenomenon. The absolute QE of the current tube was not yet measured, however we expect it to be relatively low, a consequence of a lack of potassium during one step of the photocathode process.

Fig. 5 shows the ADC spectrum for single photons at 20 kV, together with the dark noise distribution. The spectrum was fitted to a Gaussian plus exponential curve allowing to visualize the fraction of back scattered electrons. The fit indicates that about 50% of the 20 kV electrons are back scattered and deposit therefore only part of their energy in the crystal. This value and the shape of the spectrum are in good agreement with measured back scattering data [11]. The ratio width-to-peak of the Gaussian component is about 25%, supporting the M.C. calculations. Calibration of the ADC scale to photoelectons gives a peak position of 34.4 pe. The photoelectric yield as a function of the applied HV – positive and negative – is shown in Fig.6. The tube was exposed to single photons hitting the tube from the top (90°), with a contribution of double photons of less than 10%. In both powering schemes, the tube could be operated well above 20 kV. Below about 7 kV no photoelectrons could be detected. The photoelectric yield at 20 kV, i.e. the primary gain of the anode, was 40 for negative HV and about 15% lower for negative HV. We attribute the lower yield measured with positive HV to an optical effect in the region of the window/light guide interface related to liquid per-fluor hexane (C_6F_{14}) which we used as dielectric insulator in this case. The photoelectric yield was measured for three different polar angles ($0°, 45°$ and $90°$). We found the yield to scale like $1 : 1.1 : 4.1$ in good agreement with the M.C. results (Fig. 3). Also the absolute yields agree within 15% with the Geant4 calculations if one applies the detection efficiency of the PMT which was estimated to 22.5%.

The dark count rate was determined by delaying the gate of the ADC w.r.t. the trigger by 400 ns. For positive HV, dark noise rates as low as 100 kHz at a threshold of 0.1 p.e. (10 kHz, 1 p.e.) were obtained, while for negative HV the values are higher by typically a factor 20, indicating the existence of micro discharges between the corrector electrode and the base flange. Normalizing the noise rates to the photocathode surface (1020 cm^2) results in values between 100 and 10 $\mathrm{Hz/cm}^2$ (at about $T = 25°$).

The timing performance of the tube was assesed in a prelimiary way at 20 kV. The time distribution shows a tail to longer times. Its width is 2.5 ns (FWHM) after subtraction of the time jitter of the LED.

5. Summary and outlook

We report about design, fabrication and test of a first fully operational X-HPD tube with conical LYSO crystal anode. Since its production two months ago, the tube operated very stably up to 25 kV, a value which can probably still be increased by improving the electrical insulation. The 'double cathode' effect observed in a previous prototype tube was confirmed. The tube shows a primary gain of up to 40 at 20 kV. The absolute value and the angular dependence of the gain are in good agreement with Geant4 calculations modelling the light transport in the anode assembly. When powered with positive HV, the tube has a very low dark noise rate (100 $\mathrm{Hz/cm}^2$ at 0.1 p.e.). The time resolution of 2.5 ns (FWHM) appears already adequate for water Cherenkov applications. The Monte-Carlo simulations, validated by our measurements, allow studying alternative anode configurations which may lead to better performance in terms of signal definition and time resoultion, and further simplified and cost effective designs, optimized

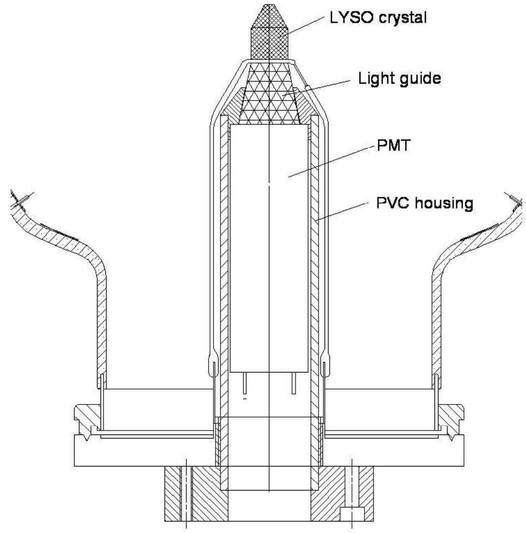

Fig. 1. Drawing of the X-HPD crystal anode assembly.

for large volume production.

Acknowledgments

We would like to thank our technical staff at CERN, C. David and M. v. Stenis, for their competent and dedicated support in preparing the HPD components and test equipment. We are grateful to G. Hallewell (CPPM Marseille) for his continuous interest and support of this project.

References

[1] A. Ball et al., *C2GT : intercepting CERN neutrinos to Gran Sasso in the Gulf of Taranto to measure* θ_{13}, Eur. Phys. J. C (2007).

[2] G. van Aller et al., *A "smart" 35cm Diameter Photomultiplier.* Helvetia Physica Acta,**59**, (1986) 1119 ff.

[3] R. Bagduev et al., Nucl. Instr. Meth. **A 420** (1999) 138.

[4] D. Ferenc, D. Kranich, A. Laille and E. Lorenz, *The novel Light Amplifier concept.* Nucl. Instr. Meth. **A 567** (2006) 166.

[5] G. Hallewell, *Crystal-based hybrid single photon detector development for the KM3NeT cubic kilometre neutrino telescope.* Proceedings of the *International Workshop on a Very Large Volume Neutrino Telescope for the Mediterranean Sea*, April 2008, to be published in NIM **A**.

[6] A. Braem, C. Joram, F. Piuz, E. Schyns and J. Seguinot, *Technology of photocathode production*, Nucl. Instr. and Meth. **A 502** (2003) 205.

[7] A. Braem et al., Nucl. Instr. Meth. **A 570** (2007) 467.

[8] A. Braem et al., Nucl. Instr. Meth. **A 581** (2007) 469.

[9] S. Agostinelli et al., *GEANT4 – a simulation toolkit*, Nucl. Instr. Meth. **A 506** (2003) 250.

[10] A. Braem et al., Proceedings of the *International Workshop on a Very Large Volume Neutrino Telescope for the Mediterranean Sea*, April 2008, to be published in NIM **A**.

[11] E.H. Darlington, *Backscattering of 10-100 keV electrons from thick targets*, J. Phys. D, Vol. 8, (1975) 85-93

Fig. 2. Photo of the X-HPD with conical LYSO crystal anode.

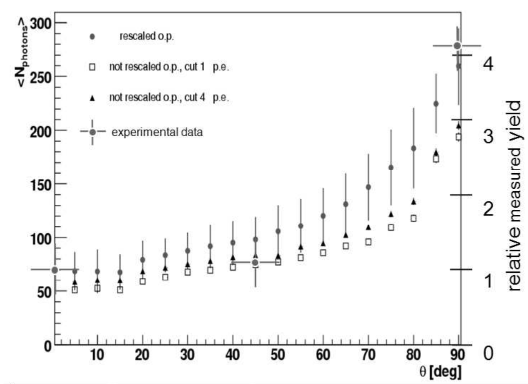

Fig. 3. Results of the Geant4 simulations for three different anode geometries. The number of detectable photons for an incident electron of 20 keV energy are plotted versus the incidence angle.

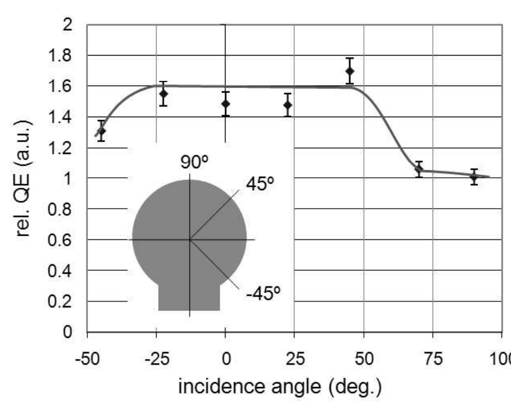

Fig. 4. Variation of the relative quantum efficiency (at 420 nm) as function of the angle of incidence on X-HPD. The line is drawn by hand to guide the eye.

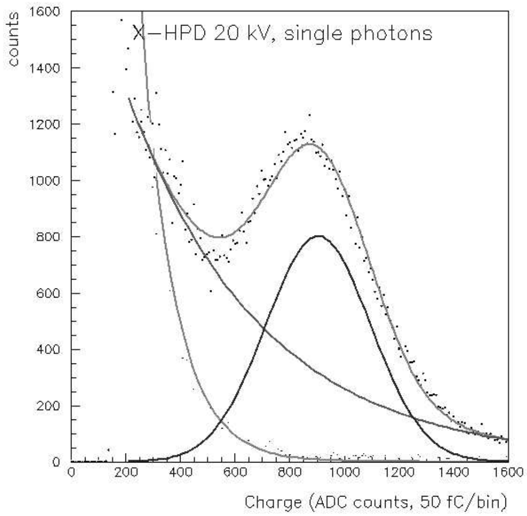

Fig. 5. Charge spectrum for single photons at $U_acc = +20$ kV. The dark noise spectrum, which is also shown, has been subtracted. A small contribution of the second photoelectron is visible.

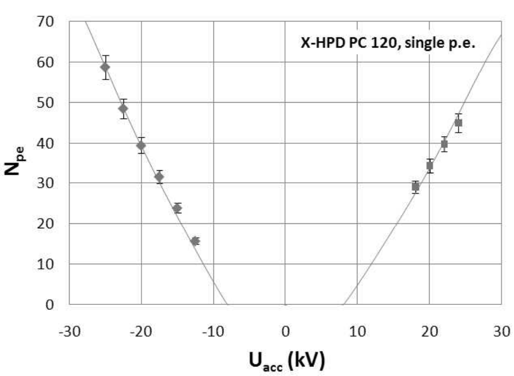

Fig. 6. Photoelectric yield vs. U_acc for positive and negative HV.